THE ASTROPHYSICAL JOURNAL, 235:386–391, 1980 January 15

RELATIVISTIC JETS AND THE CONTINUUM EMISSION IN QSOs

ALAN P. MARSCHER
Department of Physics, University of California, San Diego
Received 1979 April 6; accepted 1979 July 30

ABSTRACT

The radio through optical, and possibly X-ray, emission of QSOs and active galactic nuclei is interpreted in terms of a relativistic jet containing high-energy particles and magnetic field. An observer whose line of sight is nearly parallel to the jet axis detects a strong, compact radio source whose flux density smoothly connects with an optical spectrum which is much steeper than that emitted in the rest frame of the jet flow. The radiation is strongly polarized, and this type of source is identified with the optically violent variables. Larger viewing angles relative to the jet axis result in spectral dominance by the central region containing the "energy machine" which drives the energy flux in the jet. This radiation is weakly polarized, has a flatter spectrum and low degree of variability, and is associated with much weaker radio sources. These results are found to be consistent with presently available observational data and future observational tests are suggested. For example, the source size, as inferred from variability time scales, must increase with wavelength in the optical-infrared portion of the spectrum.

Subject headings: BL Lacertae objects — quasars — X-rays: sources

I. INTRODUCTION

Recent observations of the high-frequency radio (1–100 GHz; hereafter referred to as "radio") and infrared to optical (10^{14}–10^{15} Hz; hereafter referred to as "optical") emission from QSOs, BL Lacertae objects, and active galactic nuclei, suggest that the radio and optical properties in some of these objects are strongly correlated (O'Dell *et al.* 1978; Owen *et al.* 1978; Condon, Jauncey, and Wright 1978; Machalski and Condon 1979). In particular, the spectra of those sources with strong radio emission tend to suggest a smooth transition from the generally flat radio regime to the steeper optical continuum (Condon 1978). Furthermore, the extremely active "optically violent variables" (OVVs) have been found to possess the following properties: high degrees of optical linear polarization (e.g., Stein 1978; Stockman 1978), steeper than average optical spectral indices (Visvanathan 1973; Kinman 1975; Stein, O'Dell, and Strittmatter 1976), and associated strong, variable, flat spectrum, compact radio sources (Stein 1978; Kellermann and Pauliny-Toth 1969). It thus appears that, at least in certain classes of objects, there is a physical connection between the optical and radio emitting regions which should be addressed by any model for the radiation observed at either range of frequencies.

Although the radio emission from QSOs and similar objects appears to be adequately explained by the incoherent synchrotron process (e.g., Kellermann and Pauliny-Toth 1969), the variability observed in most compact radio sources at first glance seems to be inconsistent with this view (e.g., Burbidge, Jones, and O'Dell 1974; Marscher *et al.* 1979). This problem and the observed apparent superluminal expansions in some sources (Cohen *et al.* 1977) (both of which assume cosmological distances) can best be explained in terms of relativistic phase effects or bulk motion of one or more radio components (e.g., O'Dell 1978; Christiansen, Scott, and Vestrand 1978; Blandford, McKee, and Rees 1977). The most recent VLBI results (Readhead *et al.* 1979) suggest that the radio emission may arise from regions inside relativistic jets which emanate from the innermost central volumes of these objects. Prior to these observations, such a scenario had been proposed theoretically by Blandford and Rees (1978) and Blandford and Königl (1979).

Here we show that the relativistic jet model can explain the association of OVVs with strong, variable radio sources, strong optical polarization, and continuity of the radio to optical spectra. This study complements the conclusions of Scheuer and Readhead (1979), who find that the relativistic jet model satisfactorily accounts for the large percentage of radio-quiet QSOs. It also represents an alternative to a similar (but weaker) statistical correlation of the above properties suggested in the model of Blandford and Königl (1979).

II. PROPERTIES OF A RELATIVISTIC JET

Relativistic beams in radio sources were first postulated by Blandford and Rees (1974) to explain the apparent continuous supply of energy from the nucleus of a radio galaxy to its outer radio lobes. The reader should refer to their paper for a discussion of the detailed physics associated with a relativistic jet. Figure 1 illustrates the basic properties of such a jet. A region of intense particle acceleration is imagined to exist at the extreme central region of the object. A confining plasma surrounds this "energy machine", and the plasma is assumed to possess steeper pressure and density gradients along a given axis (presumably the rotational axis) than perpendicular to it. The

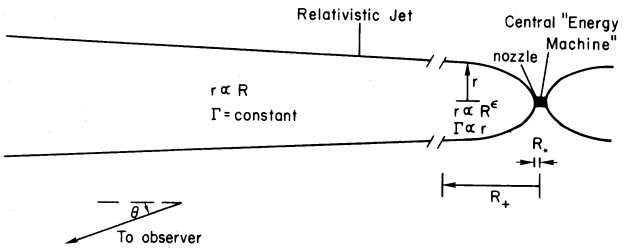

FIG. 1.—Schematic representation (not to scale; in particular note the change in scale at $R \sim R_+$) of a source containing two oppositely directed relativistic jets. After Blandford and Rees (1974, 1978).

pressure anisotropies cause the relativistic material to stream out in two directions along this axis. A "nozzle" is set up at radius R_* where the flow becomes supersonic (Lorentz factor $\Gamma_* = 1.22$). Beyond this region the flow accelerates, and the width of the beam r broadens rather slowly with radius R. At some radius R_+ the protons become nonrelativistic and the flow is inertial. If the jet is "free" at this point (i.e., there is no confining external pressure), then $r \propto R$, i.e., the flow is in a cone of constant opening angle.

We now discuss the physical conditions in each of the main three regions of flow (see Blandford and Rees 1974 for details).

1) $R < R_*$. Inside the central "energy machine" we expect a highly turbulent situation with a consequently disordered magnetic field. As the relativistic plasma proceeds down the channel, however, the field begins to become stretched out along the direction of flow. The magnetic field strength and relativistic particle density and internal energy increase due to compression as the nozzle is approached.

2) $R_+ > R > R_*$. Beyond the "nozzle" the flow is accelerated by the conversion of internal relativistic particle energy (represented by an individual electron's Lorentz factor γ_e) to bulk kinetic energy, so that the bulk Lorentz factor $\Gamma \propto \gamma_e^{-1} \propto r$. The channel width r depends rather weakly on the pressure gradient; we thus also expect r to increase slowly with radius R. For a power law pressure gradient $r \propto R^\epsilon$, with ϵ small. Here, following Reynolds and McKee (1979), we adopt $\epsilon \sim 0.2$. The magnetic field is stretched out along the direction of flow, with a radial dependence $B \propto r^{-2} \propto R^{-2\epsilon}$. (If the jet carries a net current, however, a substantial azimuthal component to the field may arise; see, e.g., Benford 1978. We do not consider this situation here.) If the relativistic electrons have a power law energy distribution

$$N(\gamma_e) = N_0 \gamma_e^{-s} [\gamma_1(R) < \gamma_e < \gamma_2(R)] , \tag{1}$$

then, since the density $n \propto \Gamma^{-1} r^{-2} \propto R^{-3\epsilon}$, $N_0 \propto r^{-(s+2)} \propto R^{-\epsilon(s+2)}$ (for $\beta \approx 1$).

3) $R > R_+$. Beyond R_+ the protons are subrelativistic in the rest frame of the flow and the bulk Lorentz factor "freezes out" at a value $\sim \Gamma_+ \equiv \Gamma(R_+)$. If the external pressure remains sufficient to confine the jet, then the channel width broadens somewhat more rapidly with radius, $\epsilon(R > R_+) \to 1.5\epsilon(R < R_+)$. We assume here that the jet becomes "free" at R_+; this simplification is demanded by the radio observations, which show a source width $\gg \Gamma_+ R_*$ (see § IV).[1] In this case $r \propto R$, and the Lorentz factors of the electrons (which still have relativistic internal energies) fall adiabatically as $\gamma_e \propto r^{-2/3} \propto R^{-2/3}$. A substantial perpendicular component of the magnetic field may arise, in which case $B \propto R^{-1}$. The radial dependence of the electron energy spectrum coefficient is $N_0 \propto R^{-2(s+2)/3}$ in this region.

III. THE SYNCHROTRON SPECTRUM

Except in the extreme central region near the "energy machine" ($R < R_*$), the source is inhomogeneous in the sense that the magnetic field, electron energies, and electron density all decrease with increasing radius. Similar synchrotron emitters have been studied previously by Slysh (as reported by Shklovsky 1970), Condon and Dressel (1973), de Bruyn (1976), and Marscher (1977), who find that such a geometry tends to flatten significantly the partially opaque radio spectrum. This effect is mainly due to an inverse proportionality of apparent source size with frequency. As we show below, this same effect can result in a steepening of the transparent optical spectrum in QSOs where the observer's line of sight lies almost parallel to the axis of the relativistic jet.

a) Individual Regions

1) $R < R_*$.—Since the magnetic field and density do not decrease substantially within the "nozzle" radius, the spectrum arising from the innermost region should resemble that of a homogeneous synchrotron source:

$$S_\nu \propto \nu^{-(s-1)/2} \quad (\nu_2 > \nu \gg \nu_m) \tag{2}$$

$$S_\nu \propto \nu^{5/2} \quad (\nu \ll \nu_m) , \tag{3}$$

[1] If the jet becomes free before the internal energies of the protons become nonrelativistic, say at radius R_f, the half-width of the jet will increase rapidly with R from a value r_f to $\gamma_{pf} r_f$, where γ_{pf} is the mean Lorentz factor of the protons at R_f. Beyond this point ($R = R_+$, which is likely to be very close to R_f), the flow is inertial with constant Lorentz factor.

where ν_m is the synchrotron self-absorption turnover frequency. The spectrum cuts off for frequencies greater than the critical frequency of the highest energy electron,

$$\nu_2 \approx 2.8 \times 10^6 B\gamma_2^2 . \tag{4}$$

In the presence of a magnetic field, synchrotron losses cause a cutoff to occur in the spectrum above a rest frequency

$$\nu_2(R_*) \approx 10^8 B^{-3}(R_*) R_{*\mathrm{pc}}{}^{-2}\Gamma_*{}^2\beta_*{}^2 \tag{5}$$

near the nozzle (where no relativistic particle injection is assumed to occur). (The pitch angle distribution is assumed to re-isotropize in the flow frame on a time scale $\ll \Gamma_*{}^{-1}R_*/c$.) As we see below in the specific case of 3C 345, $\nu_2(R_*)$ most likely lies in the optical-ultraviolet portion of the electromagnetic spectrum.

2) $R_+ > R > R_*$.—In this segment of the jet the magnetic field and relativistic electron density and energies decrease with radius. This has two major effects on the synchrotron emission: a gradient in the maximum electron energy and thus in the high-frequency cutoff ν_2, and a radial dependence of the volume emission and absorption coefficients at any given observer's frequency. Synchrotron losses yield a radial variation of the maximum electron Lorentz factor

$$\gamma_2(R) \approx \gamma_2(R_*)[B(R_*)/B(R)]^2[(\beta\Gamma)/(\beta_*\Gamma_*)](R_*/R) \approx \gamma_2(R_*)(R_*/R)^{1-5\epsilon} \tag{6}$$

as long as $\epsilon < 0.2$, while adiabatic expansion losses give

$$\gamma_2(R) = \gamma_2(R_*)(R_*/R)^{\epsilon} . \tag{7}$$

Note that expansion losses dominate for $\epsilon > \frac{1}{6}$ while synchrotron losses determine γ_2 for $\epsilon < \frac{1}{6}$. The observed cutoff frequency ν_2 is directly proportional to the Doppler factor of the relativistic flow, δ, which depends on the observer's angle of sight θ ($\theta = 0$ along the axis of the jet):

$$\begin{aligned} \delta = \Gamma^{-1}(1 - \beta\cos\theta)^{-1} &\propto \Gamma \propto R^{\epsilon} \qquad (\theta \lesssim \Gamma^{-1}) \\ &\propto \Gamma^{-1} \propto R^{-\epsilon} \quad (\theta \gtrsim \Gamma^{-1}) . \end{aligned} \tag{8}$$

The high-frequency cutoff therefore follows the relation

$$\begin{aligned} \nu_2 \approx 2.8 \times 10^6 B(R)\gamma_2{}^2(R)\delta &\propto R^{-(2-9\epsilon)} \quad (\theta \lesssim \Gamma^{-1}, \epsilon \le \tfrac{1}{6}) \\ &\propto R^{-(2-7\epsilon)} \quad (\theta \gtrsim \Gamma^{-1}, \epsilon \le \tfrac{1}{6}) \\ &\propto R^{-3\epsilon} \qquad (\theta \lesssim \Gamma^{-1}, \epsilon \ge \tfrac{1}{6}) \\ &\propto R^{-5\epsilon} \qquad (\theta \gtrsim \Gamma^{-1}, \epsilon \ge \tfrac{1}{6}) , \end{aligned} \tag{9}$$

and the effective maximum radius $R_m(\nu)$ decreases with frequency. (*Note*.—This equation and those that follow are strictly valid only for disordered fields. We expect them to approximately hold as long as the observed linear polarization does not exceed 10–20%.) We can obtain the observed flux density by integrating over radius R. An exact relation can be obtained for $\theta = 0$ and $\theta = \pi/2$ which we expect to be approximately valid for $\theta \lesssim \Gamma^{-1}$ and $\theta \gg \Gamma^{-1}$, respectively:

$$\begin{aligned} S_\nu &\propto \nu^{-(s-1)/2} \int_{R_*}^{R_m(\nu)} N_0 B^{(s+1)/2} r^2 \delta^{(3+s)/2} dR \\ &\propto R_m{}^{1-\epsilon(3s-1)/2} \nu^{-(s-1)/2} \propto \nu^{\alpha} \quad (\theta \lesssim \Gamma^{-1}) \end{aligned} \tag{10}$$

with

$$\begin{aligned} \alpha &= -(s-1)/2 - [1 - \epsilon(3s-1)/2]/(2 - 9\epsilon) \quad (\epsilon \le \tfrac{1}{6}) \\ &= -(1-\epsilon)/(3\epsilon) \qquad\qquad\qquad\qquad (\epsilon \ge \tfrac{1}{6}) . \end{aligned} \tag{11}$$

These expressions for α are valid for $\nu_2(\Gamma_+) < \nu < \nu_2(\Gamma_*)$ and $\theta \lesssim \Gamma^{-1}$. For $\nu_m(\Gamma_+) < \nu < \nu_2(\Gamma_+)$, $\alpha = -(s-1)/2$. (See Ozernoy and Sazonov 1968 for the relations for the emission and absorption coefficients used here for a relativistic jet.) The situation is more complex for higher line-of-sight angles θ:

$$S_\nu \propto [R^{1-5\epsilon(s+1)/2}]_{R_*}^{R_m(\nu)} \nu^{-(s-1)/2} \quad (\theta \gg \Gamma^{-1}) . \tag{12}$$

If $\epsilon > 2(s+1)^{-1}/5$, the observed flux is produced mainly at small radii, i.e., near the nozzle radius R_*. We expect this to be valid for what we consider likely "typical" values of ϵ and s: $\epsilon \approx 0.2$ and $s \gtrsim 1.5$. Therefore, the

shape of the spectrum observed at high inclination angles $\theta \gg \Gamma^{-1}$ reflects the "native" spectrum as emitted in the rest frame of the source.

However, the situation is completely different for lines of sight nearly parallel to the jet (see eq. [11]). The nonuniformity of the source causes the observer to measure a much *steeper* spectrum than that given by the electron energy spectrum ($\alpha = -(s-1)/2$). Furthermore, the spectral slope depends mainly on the geometry of the source through the parameter ϵ. For example, for $\epsilon = \frac{1}{6}$, the observed spectral index α is $-5/3$. A higher value of ϵ results in a flatter spectrum, but note that in this case α is independent of the slope of the relativistic electron spectrum s (see eq. [11]).

The variation of the synchrotron self-absorption optical depth $\tau(\nu)$ with radius is also important:

$$\begin{aligned}\tau(\nu) &\propto N_0 B^{(s+2)/2} l \delta^{(s+2)/2} \nu^{-(s+4)/2} \\ &\propto R^{1-3\epsilon(2+s)/2} \nu^{-(s+4)/2} \quad (\theta \lesssim \Gamma^{-1}) \\ &\propto R^{-\epsilon(8+5s)/2} \nu^{-(s+4)/2} \quad (\theta \gg \Gamma^{-1}), \end{aligned} \tag{13}$$

where l is the path length through the source: $l \sim R$ for $\theta \lesssim \Gamma^{-1}$ and $l \sim r$ for $\theta \gg \Gamma^{-1}$. For lines of sight along the jet ($\theta \lesssim \Gamma^{-1}$) the turnover frequency ν_m (corresponding to $\tau \sim 1$) varies as $R^{-\eta}$ where $|\eta| \lesssim 0.1$ for $\epsilon \approx 0.2$ and $1.5 \lesssim s \lesssim 2.5$. Therefore, one expects that a frequency at which radiation is optically thin at radius R_+ will also lie above the turnover ν_m at smaller radii. This implies that the turnover frequency of the spectrum as a whole is simply $\nu_m(R_+)$. This may not, however, be the case for viewing angles $\theta \gg \Gamma^{-1}$. Instead, for $\epsilon > 2(s+1)^{-1}/5$ (the flux is dominated by contributions at radii near R_+ for lower values of ϵ), the spectrum is partially opaque (i.e., $2.5 > \alpha > 0$) below the turnover frequency corresponding to the nozzle radius R_*, $\nu_m(R_*)$. The value of the spectral index can be straightforwardly calculated (see, e.g., de Bruyn 1976):

$$\alpha = -(s-1)/2 + [5\epsilon(s+1)/2 - 1](s+4)/[\epsilon(8+5s)] \quad [\epsilon > 2(s+1)^{-1}/5, \nu \ll \nu_m(R_*)]. \tag{14}$$

For $\epsilon \approx 0.2$ and typical values of s, this partially opaque spectrum is quite flat, $\alpha \approx 0.2$–0.5. These high θ jets are associated with weak radio sources (Scheuer and Readhead 1979), and these sources should therefore have quite small effective VLBI dimensions ($R \sim R_*$) near the turnover frequency.

3) $R > R_+$.—The physical parameters in this region fall off rather rapidly with radius (see § II). The main contribution to the optically thin flux density therefore arises from the innermost radii of the region, $R \sim R_+$. The radius where the optical depth is unity, however, varies with frequency such that the partially opaque spectral index is (independent of the line of sight since Γ is constant)

$$\begin{aligned}\alpha &= -(s-1)/2 + 3.5(s-1)(s+4)/(7s+8) \quad (B \propto R^{-1}) \\ &= -(s-1)/2 + 0.5(5s-2)(s+4)/(5s+7) \quad (B \propto R^{-2}), \end{aligned} \tag{15}$$

which, for typical values of s, ranges from 0.27 ($s = 1.5$, $B \propto R^{-1}$) to 1.0 ($s = 2.5$, $B \propto R^{-2}$).

b) Overall Spectrum

The radio, optical, and possibly X-ray synchrotron spectrum is qualitatively illustrated in Figure 2. The radio emission arises from the $R \sim R_+$ region for $\theta \lesssim \Gamma_+^{-1}$ and from $R \sim R_*$ for larger θ. The optically thin millimeter to far-infrared emission from $\nu_m(R_+)$ to $\nu_2(R_+)$ has a spectral index $\alpha = -(s-1)/2$ and arises mainly from radii $R \sim R_+$ for the $\theta \lesssim \Gamma^{-1}$ case. At higher line-of-sight angles all optically thin emission is dominated by contributions from the innermost radii, $R \lesssim R_*$, and have spectral indices $\alpha = -(s-1)/2$. For the $\theta \lesssim \Gamma^{-1}$ case, the spectrum steepens to a slope given by equation (11) from $\nu_2(R_+)$ to $\nu_2(R_*)$. Beyond $\nu_2(R_*)$ it flattens again to $\alpha = -(s-1)/2$ unless cut off by, say, synchrotron losses (see eq. [5]).

We expect the turbulent region containing the "energy machine" to produce a certain fraction of the optical flux (with a relatively flat spectral index $\alpha = -(s-1)/2$). However, the theory of energy flow from this region to the jet has not yet been sufficiently developed to predict the percentage of the total flux contributed by this innermost region. Nevertheless, we expect the relativistic jet component to dominate this central source only when θ is sufficiently small ($\theta \lesssim \Gamma^{-1}$) that the relativistic beaming factor ($S_\nu \propto \delta^{(s+3)/2}$) enhances the observed jet emission (see also Blandford and Königl 1979). Therefore, contrary to the opinions expressed at the 1978 Pittsburgh BL Lac Conference (e.g., Stein 1978; Blandford and Rees 1978; Miller and French 1978), according to this model it is the radio-quiet, relatively quiescent optical sources, and not the BL Lac type variables, which might display emission that originates close to the ultimate energy source. We speculate that the higher degree of variability observed in the OVVs may be due to the probable small change in source parameters required to vary the energy flow in the jet relative to that needed to change the luminosity of the "energy machine," which is thought to remain fairly stable for over 10^6 years. It is also possible that a more diffuse "halo" component contributes a significant fraction of the quiescent optical flux.

Note also that it is possible for a steep-spectrum optical source to possess an X-ray component which, although

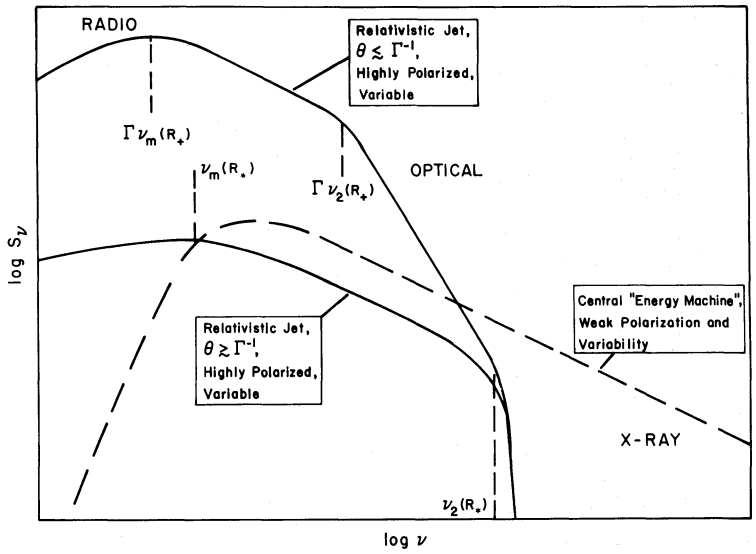

FIG. 2.—Schematic example of an electromagnetic spectrum observed from a source containing a relativistic jet. Note the difference in the fraction of flux contributed by the jet as the viewing angle θ changes. Extension of the "energy machine" spectrum into X-ray energies is speculative.

a natural extension of the optical spectrum, has a flat spectral index similar to that of the transparent radio source. Such X-ray sources therefore need not arise from Compton scattering of the radio photons, and variations should be more closely correlated with optical than radio outbursts, with characteristically short (viz., days to months) time scales.

c) *Polarization*

Figure 2 gives the expected linear polarization properties in different regions of the spectrum. The relatively quiescent optical, radio-quiet, object should be only weakly polarized, since this emission originates in the highly turbulent central volumes of the source (or in a "halo") where the magnetic field is most likely highly disordered. The active, steep-spectrum objects should display strong optical polarization with a position angle indicating a magnetic field stretched out along the jet. (If the jet carries a current, a more complex field geometry might occur; see Benford 1978.) However, recent observations have shown that compact radio jets are curved (most likely due to projection effects; Readhead *et al.* 1978), so that it is difficult to predict the alignment of the field relative to the observed radio axis. The radio emission should also be polarized, although the possibility of a magnetic field transverse to the flow for either the jet component (see § II) or a shock wave component (see Blandford and Königl 1979) again complicates any prediction of the observed position angle relative to the radio structure.

IV. DISCUSSION

In the previous sections we have been relatively ambitious in showing that the relativistic jet model of QSOs can explain the qualitative features of the radio to optical spectra of these and similar objects. In this section we become somewhat more quantitative and then suggest ways in which the model can be observationally tested.

A good source to examine for a quantitative analysis is 3C 345, which has been well observed at both radio and optical frequencies. VLBI observations (e.g., Cohen *et al.* 1977) detect apparent superluminal expansion of the radio source at a speed $\sim 7c$, which, in the context of relativistic jets requires $\Gamma_+ \gtrsim 7$; we adopt $\Gamma_+ = 7$. The projected component sizes are ~ 4 and 7 pc (Shaffer *et al.* 1977; $H_0 = 55$ km s^{-1} Mpc^{-1}, $q_0 = 0$; we analyze the 7 pc component), which corresponds to $R_+ \sim 50$ pc for a viewing angle $\theta \sim \Gamma_+{}^{-1}$. The optical spectral index $\alpha = 1.5$ (Oke, Neugebauer, and Becklin 1970) indicates $\epsilon = 0.18$ (eq. [11]), so that $R_* \sim R_+(\Gamma_+/\Gamma_*)^{-1/\epsilon} \sim 3 \times 10^{-3}$ pc, which is of the order of 4 light-days. This is consistent with the reported optical variability on time scales of ~ 10 days (Kinman 1968).

The magnetic field in the radio jet component is $\sim 2 \times 10^{-3}$ gauss (from data of Shaffer *et al.*; see, e.g., Marscher *et al.* 1979 for the relevant equations). The magnetic field at the nozzle radius $R_*(B \propto R^{-2\epsilon})$ is then ~ 0.1 gauss. We therefore do not expect synchrotron losses (see expression [5]) to affect the results of § III below $\sim 10^{16}$ Hz. The synchrotron cutoff may, however, lie at lower optical frequencies in other sources and could then be responsible for the extremely steep, curved spectra sometimes seen (e.g., Stein 1978).

The detailed nature of flux variations in OVVs can serve as a strict observational test of this model. Since the size of the emitting region at optical frequencies is a strong function of radius R (see relation [9]), the variations

should occur first at the higher frequencies with correspondingly shorter characteristic variational time scales. For example, for $\epsilon = 0.2$, $R \propto \nu^{-4/3}$, $R \sim \Gamma^2 ct$ (Rees 1967), and $\Gamma \propto R^{0.2}$, so that the time scale $t_{\rm var} \propto \nu^{-0.8}$. (This should only hold for flux changes on very short time scales $\lesssim R_*/c$; see below.) Simultaneous, short-term ($\lesssim 1$ week) flux monitoring at optical and infrared wavelengths could therefore be used to test the theory.

Since the spectral index at optical frequencies of OVVs should be determined mainly by the structure of the source, long-term ($t_{\rm var} \gg R_*/c$) variations should not be accompanied by significant changes in spectral index, except perhaps in the case of a steepening due to synchrotron losses in a higher magnetic field. This is consistent with the behavior of OVVs observed to date (Visvanathan 1973; Stein 1978).

Since the relativistic jets should be aligned with any extended, double radio lobes, this model predicts that the OVV phenomenon should not occur when this classical, well-separated double structure appears (implying $\theta \gg \Gamma^{-1}$) (see also Scheuer and Readhead 1979).

If this model is found to survive these observational tests, it would be interesting to try to relate it to the geometry of the emission-line regions in QSOs. An observational relation has been discovered by Miley and Miller (1979), who find that extended double radio structure (corresponding to large θ) is associated with broader emission-line widths than is the case for compact radio sources (small θ). Motion of the emission-line clouds directed mainly perpendicular to the jet could account for this effect.

The author thanks Drs. S. L. O'Dell and A. M. Wolfe for useful discussions. Extragalactic research at UCSD is supported by NASA and the NSF.

REFERENCES

Benford, G. 1978, *M.N.R.A.S.*, **183**, 29.
Blandford, R. D., and Königl, A. 1979, *Ap. J.*, **232**, 34.
Blandford, R. D., McKee, C. F., and Rees, M. J. 1977, *Nature*, **267**, 211.
Blandford, R. D., and Rees, M. J. 1974, *M.N.R.A.S.*, **169**, 395.
———. 1978, in *Pittsburgh Conference on BL Lac Objects*, ed. A. M. Wolfe (Pittsburgh: University of Pittsburgh Press), p. 328.
Burbidge, G. R., Jones, T. W., and O'Dell, S. L. 1974, *Ap. J.*, **193**, 43.
Christiansen, W. A., Scott, J. S. and Vestrand, W. T. 1978, *Ap. J.*, **223**, 13.
Cohen, M. H. *et al.* 1977, *Nature*, **268**, 405.
Condon, J. J. 1978, in *Pittsburgh Conference on BL Lac Objects*, ed. A. M. Wolfe (Pittsburgh: University of Pittsburgh Press), p. 21.
Condon, J. J., and Dressel, L. L. 1973, *Ap. Letters*, **15**, 203.
Condon, J. J., Jauncey, D. L., and Wright, A. E. 1978, *A.J.*, **83**, 1036.
de Bruyn, A. G. 1976, *Astr. Ap.*, **52**, 439.
Kellermann, K. I., and Pauliny-Toth, I. I. K. 1969, *Ap. J. (Letters)*, **155**, L71.
Kinman, T. D. 1968, *Science*, **162**, 1081.
———. 1975, in *IAU Symposium 67, Variable Stars and Stellar Evolution*, ed. V. E. Sherwood and L. Plaut (Dordrecht: Reidel), p. 573.
Machalski, J., and Condon, J. J. 1979, *A.J.*, **84**, 164.
Marscher, A. P. 1977, *Ap. J.*, **216**, 244.
Marscher, A. P., Marshall, F. E., Mushotzky, R. F., Dent, W. A., Balonek, T. J., and Hartman, M. F. 1979, *Ap. J.*, **233**, 498.
Miley, G. K., and Miller, J. S. 1979, *Ap. J. (Letters)*, **228**, L55.
Miller, J. S., and French, H. B. 1978, in *Pittsburgh Conference on BL Lac Objects*, ed. A. M. Wolfe (Pittsburgh: University of Pittsburgh Press), p. 228.
O'Dell, S. L. 1978, in *Pittsburgh Conference on BL Lac Objects*, ed. A. M. Wolfe (Pittsburgh: University of Pittsburgh Press), p. 312.
O'Dell, S. L., Puschell, J. J., Stein, W. A., Owen, F., Porcas, R. W., Mufson, S., Moffett, T. J., and Ulrich, M.-H. 1978, *Ap. J.*, **224**, 22.
Oke, J. B., Neugebauer, G., and Becklin, E. E. 1970, *Ap. J.*, **159**, 341.
Owen, F. N., Porcas, R. W., Mufson, S. L., and Moffett, T. J. 1978, *A.J.*, **83**, 685.
Ozernoy, L. M., and Sazonov, V. N. 1968, *Nature*, **219**, 467.
Readhead, A. C. S., Cohen, M. H., Pearson, T. J., and Wilkinson, P. N. 1978, *Nature*, **276**, 768.
Readhead, A. C. S., Pearson, T. J., Cohen, M. H., Ewing, M. S., and Moffett, A. T. 1979, *Ap. J.*, **231**, 299.
Rees, M. J. 1967, *M.N.R.A.S.*, **135**, 345.
Reynolds, S., and McKee, C. F. 1979, in preparation.
Scheuer, P. A. G., and Readhead, A. C. S. 1979, *Nature*, **277**, 182.
Shaffer, D. B., *et al.* 1977, *Ap. J.*, **218**, 353.
Shklovsky, I. S. 1970, *Ap. J. (Letters)*, **159**, L77.
Stein, W. A. 1978, in *Pittsburgh Conference on BL Lac Objects*, ed. A. M. Wolfe (Pittsburgh: University of Pittsburgh Press), p. 1.
Stein, W. A., O'Dell, S. L., and Strittmatter, P. A. 1976, *Ann. Rev. Astr. Ap.*, **14**, 173.
Stockman, H. S. 1978, in *Pittsburgh Conference on BL Lac Objects*, ed. A. M. Wolfe (Pittsburgh: University of Pittsburgh Press), p. 149.
Visvanathan, N. 1973, *Ap. J.*, **179**, 1.

ALAN P. MARSCHER: Department of Physics, C-011, University of California, San Diego, La Jolla, CA 92093